Experiments on a Compact Multichannel Vector Sensor Receiver for Signal Acquisition in Underwater Communication Systems

Erjian Zhang*, Rami Rashid, Ali Abdi
Electrical and Computer Engineering Department
New Jersey Institute of Technology, Newark, NJ
ez7@njit.edu, raa62@njit.edu, ali.abdi@njit.edu

***Abstract*—Successful demodulation of transmitted signals in communication systems is highly dependent on accurate signal acquisition. In this paper, we present experimental evidence that demonstrates a ring vector receiver can remarkably improve signal acquisition, compared to a regular scalar receiver. The vector receiver measures the vector components of the underwater acoustic field, i.e., the acoustic particle velocities, in addition to the scalar component of the underwater acoustic field, that is, the acoustic pressure. The multichannel nature of the vector receiver, along with certain characteristics of the vector field components, generate stronger peaks after matched filtering, that allow for more accurate signal acquisition and packet detection.**

***Index Terms*—Signal acquisition, Underwater communication, Underwater sensing, Chirp signal, Scalar sensors, Vector sensors.**

I. Introduction

Signal acquisition is an integral part of various communication systems [1]-[5]. Usually, a chirp signal is inserted for signal acquisition at the beginning of a transmitted packet, and a matched filter is used at the receiver side to detect the starting point of the packet [6]-[8]. At the output of the matched filter, a strong peak indicates the starting point of the received packet. When the matched filter output does not provide a strong peak, especially in weak signal or strong noise scenarios, the packet may not be detected and the transmitted data can be lost.

In this paper, we propose to utilize a ring vector sensor receiver for underwater signal acquisition and packet detection. A vector sensor receiver is a multichannel device that simultaneously measures the underwater vector and scalar acoustic field components [9]. Vector sensors have been widely used for a variety of applications such as sonar, beamforming, angle of arrival estimation and source localization [10]-[14], as well as underwater communication [9], [15]-[19].

Here we focus on studying the chirp matched filtering performance of a ring vector sensor [20] receiver, and compare it with scalar sensor receivers, using experimental data. For comparison purposes, one can use physics-based [9] or statistical [21]-[23] channel models. In this paper, however, we use experimentally measured data, to examine and demonstrate the practical feasibility of the proposed approach.

The rest of this paper is organized as follows. Section II provides definitions for the vector and scalar signals. System formulations and experimental results on signal acquisition and peak detection via matched filtering using a vector receiver are presented in Sections III and IV, respectively. Concluding remarks summarizing that a vector receiver outperforms scalar receivers are given in Section V.

II. Vector and Scalar Signal Definitions

Consider Fig. 1 which shows that in response to a signal $s(t)$, a compact multichannel vector receiver in an underwater environment provides multiple signals, whereas a scalar receiver offers one signal. The signal $r(t)$ is the acoustic pressure and represents the scalar component of the field, whereas the signals $r_x(t)$, $r_y(t)$ and $r_z(t)$ are the particle velocities, i.e., the vector components of the field [9]. Let $h(t)$, $h_x(t)$, $h_y(t)$ and $h_z(t)$ represent the scalar and the x, y and z vector channel impulse responses, respectively. Then the

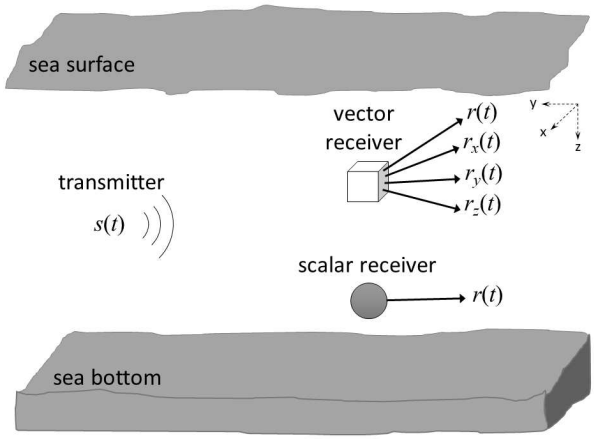

Fig. 1. Schematic representation of a multichannel vector receiver and a single channel scalar receiver and the signals they provide.

The work is supported in part by NSF, Grants IIP-1500123 and IIP-1340415.

* Currently with Shanghai Radio Equipment Research Institute, Shanghai, China.

scalar and vector signals can be written as

$$\begin{bmatrix} r(t) \\ r_x(t) \\ r_y(t) \\ r_z(t) \end{bmatrix} = \begin{bmatrix} h(t) \\ h_x(t) \\ h_y(t) \\ h_z(t) \end{bmatrix} \oplus s(t) + \begin{bmatrix} n(t) \\ n_x(t) \\ n_y(t) \\ n_z(t) \end{bmatrix}, \quad (1)$$

where $\oplus$ is convolution, and $n(t), n_x(t), n_y(t)$ and $n_z(t)$ represent the scalar and the x, y and z vector noise components, respectively. Some characteristics of the vector components are studied in [9].

Suppose one would like to perform matched filtering, for acquisition and packet detection, using the scalar signal $r(t)$. With $s(t)$ being a chirp signal, the output of the filter matched to $s(t)$ can be written as

$$r_{\text{MF}}(t) = r(t) \oplus s(T_0 - t), \quad (2)$$

where T_0 is the duration of $s(t)$. The peak at the output of the matched filter at $t = T_0$, if strong enough, can determine the beginning of a received packet. However, the peak may not be detectable in background noise, when the signal power is small or the noise power is high, as shown in the next section using experimental data. In the next section, we present experimental results on how a multichannel vector sensor can outperform a single scalar sensor, or an array of spatially separated scalar sensors, when the signal power is small.

III. Multichannel Vector Receiver Combining

Consider the four signals $r(t)$, $r_x(t)$, $r_y(t)$ and $r_z(t)$ in (1) that a vector receiver provides. Here we consider two methods to combine these signals, for improved acquisition and peak detection: selection combining and normalized combining. According to their definitions in the following subsections, these two resemble some diversity combining techniques used in wireless fading channels [6], [7], [24], [25].

A. Selection Combining

Let $P = \overline{r^2(t)}$ and $P_i = \overline{r_i^2(t)}$, $i = x, y, z$, represent average powers of $r(t)$, $r_x(t)$, $r_y(t)$ and $r_z(t)$ in (1), respectively, where by definition we have $\overline{w(t)} = T_0^{-1} \int_{T_0} w(t)dt$. Also let $r_m(t)$ be the signal that has the maximum power among P, P_x, P_y and P_z. The output of the matched filter in response to this selected signal is given by

$$r_{m,\text{MF}}(t) = r_m(t) \oplus s(T_0 - t). \quad (3)$$

To study the performance of the above combiner, we transmitted one hundred chirp signals in a large pool on the university's campus. The area of the pool was 13×23≈300 m^2, and had a varied depth from 1 to 3 m, approximately. The transmitter and receivers were placed about 0.6 m below the water surface, while the distance between them was about 20 m. The first four transmitted chirps are shown in Fig. 2. The transmitted chirp parameters included the duration of $T_0 = 0.2$ s, bandwidth of 2 kHz and center frequency of 20 kHz. The spacing between each two consecutive chirps was also T_0. Fig. 3 shows the results of the experiments.

The matched filter output of a single scalar receiver (Fig. 3, top panel), included in the study as a benchmark, does not show any peak. In contrast, the matched filter response at the output of the selection combiner, collecting signals from a vector receiver, exhibits strong peaks at the expected time instants $t = T_0, 3T_0, 5T_0, \ldots$ (Fig. 3, middle panel). As a conventional approach, we also used a vertical array of spatially separated scalar receivers that provided the same number of signals as the single vector receiver. The matched filter response at the output of the selection combiner, collecting signals from a scalar array receiver, shows small peaks at the time instants $t = T_0, 3T_0, 5T_0, \ldots$ (Fig. 3, bottom panel). Possible factors behind the superior performance of the vector receiver are studied in Section IV.

B. Normalized Combining

The selection combining method uses only one signal. The normalized combining method utilizes an average of all the signals, as defined below

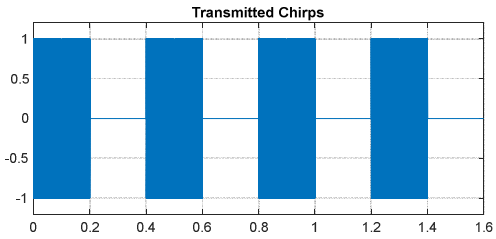

Fig. 2. The transmitted chirp signals.

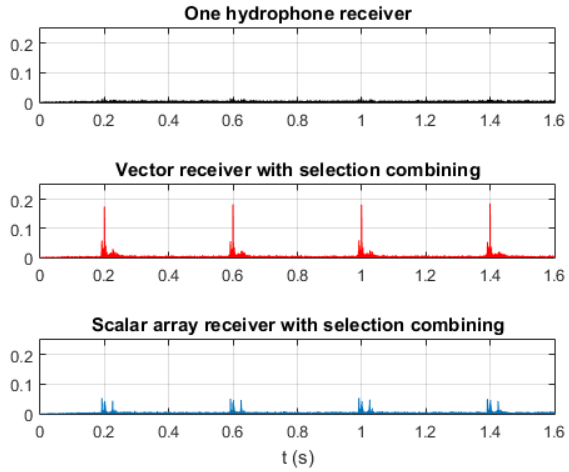

Fig. 3. The matched filter output of a selection combiner. Top: a scalar receiver (hydrophone), provided as a benchmark; Middle: a vector receiver; Bottom: a vertical array of spatially separated scalar receivers.

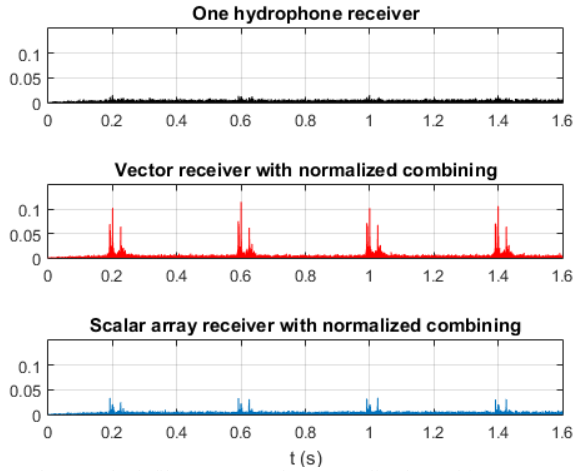

Fig. 4. The matched filter output of a normalized combiner. Top: a scalar receiver (hydrophone), provided as a benchmark; Middle: a vector receiver; Bottom: a vertical array of spatially separated scalar receivers.

$$r_a(t) = (\tilde{r}(t) + \tilde{r}_x(t) + \tilde{r}_y(t) + \tilde{r}_z(t))/4\,. \tag{4}$$

In the above equation, we have $\tilde{r}(t) = r(t)/\max_t r(t)$ and $\tilde{r}_i(t) = r_i(t)/\max_t r_i(t)$, $i = x, y, z$, where each signal is normalized by its maximum value, to bring them all within the same scale. The output of the matched filter in response to this combined signal is given by

$$r_{a,\mathrm{MF}}(t) = r_a(t) \oplus s(T_0 - t)\,. \tag{5}$$

The matched filter output of a single scalar receiver (Fig. 4, top panel) does not show any peak. In contrast, the matched filter response at the output of the normalized combiner, collecting signals from a vector receiver, demonstrates strong peaks at the expected time instants $t = T_0, 3T_0, 5T_0, \ldots$ (Fig. 4, middle panel). As a conventional approach, we also used a vertical array of spatially separated scalar receivers that provided the same number of signals as the single vector receiver. The matched filter response at the output of the normalized combiner, collecting signals from a scalar array receiver, shows small peaks at the time instants $t = T_0, 3T_0, 5T_0, \ldots$ (Fig. 4, bottom panel). In Section IV some possible reasons for the better performance of the vector receiver are provided.

Comparison of Fig. 3 and Fig. 4 reveals that there appears to be no noticeable difference between the two combining methods.

IV. Experimental Performance Studies

To understand why the vector receiver outperforms a scalar receiver and also an array of scalar receivers, in this section we look at signal-to-noise ratios (SNRs) and some possible correlations.

Fig. 5 shows multiple measurements of the SNR of the *x* and *y* vector components, as well as the SNR of the scalar component. We use a ring vector sensor receiver in our vector signal acquisition study. Given its ring geometry, it does not measure the *z* component. It has four segments on a ring, acts as two orthogonal dipoles in the *x*-*y* plane, such as those shown in Fig. 1 of [26], and therefore measures the *x* and *y* vector components (each dipole measures one vector component [26]). Signal acquisition performance of other types of vector sensors [9] can be studied following the proposed steps taken in this paper. Our scalar receivers are regular hydrophones and our transmitter is a regular projector. We observe that the SNRs of the vector components are higher than the scalar component SNRs. This can be attributed to the about 10 dB smaller noise powers of the vector components, according to the multiple noise measurements shown in Fig. 6. A theoretical explanation for the lower noise powers of a vector communication receiver can be found in [9]. Overall, higher SNRs of the vector components can explain the superior performance of the vector receiver for signal acquisition using its stronger matched filter peaks.

Measured covariance matrices of the vector receiver and an array of scalar receivers are provided in what follows, with the transmitted signal $s(t)$ being the chirp signal

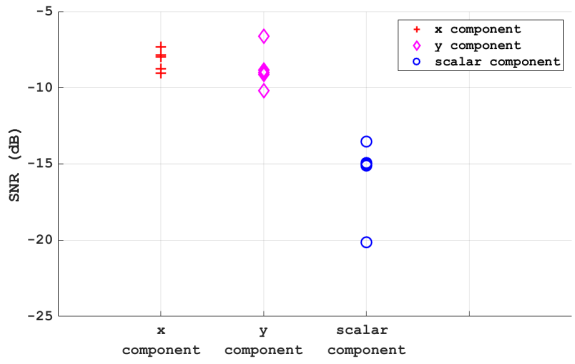

Fig. 5. Measured vector and scalar signal-to-noise ratios.

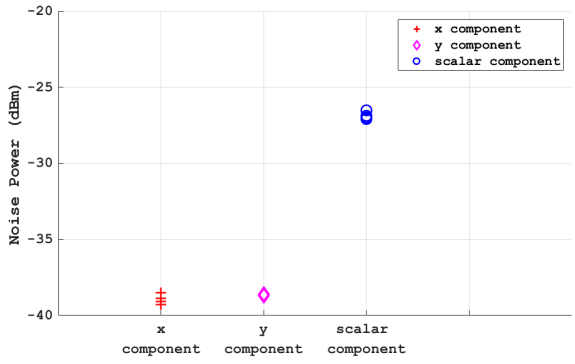

Fig. 6. Measured vector and scalar noise powers.

$$\widehat{\mathbf{C}}_{\text{vector}} = \begin{bmatrix} 1 & -0.2 & 0.1 \\ -0.2 & 1 & -0.16 \\ 0.1 & -0.16 & 1 \end{bmatrix}, \quad (6)$$

$$\widehat{\mathbf{C}}_{\text{scalar}} = \begin{bmatrix} 1 & 0.42 & 0.4 \\ 0.42 & 1 & 0.44 \\ 0.4 & 0.44 & 1 \end{bmatrix}. \quad (7)$$

Note that $\widehat{\mathbf{C}}_{\text{vector}}$ and $\widehat{\mathbf{C}}_{\text{scalar}}$ are estimates of the vector and scalar covariance matrices, respectively, of $\mathbf{C}_{\text{vector}} = E[\mathbf{r}_{\text{vector}}(t)\mathbf{r}^T_{\text{vector}}(t)]$ and $\mathbf{C}_{\text{scalar}} = E[\mathbf{r}_{\text{scalar}}(t)\mathbf{r}^T_{\text{scalar}}(t)]$, where $\mathbf{r}_{\text{vector}}(t) = [r(t)\ \ r_x(t)\ \ r_y(t)]^T$ and $\mathbf{r}_{\text{scalar}}(t) = [r_1(t)\ \ r_2(t)\ \ r_3(t)]^T$, and ^{T} stands for transpose. The signals $r_1(t)$, $r_2(t)$ and $r_3(t)$ in $\mathbf{r}_{\text{scalar}}(t)$ are the signals measured by a three-element scalar array receiver, deployed in the experiments for comparison purposes.

The smaller correlation levels in equation (6) for the vector receiver are noteworthy (some theoretical analyses can be found in [23] and [27]). By providing and utilizing less correlated signals, the vector receiver can perform as a more effective multichannel processor.

V. Conclusion

Experimental results are presented in this paper for signal acquisition in underwater communication systems, using a ring vector sensor receiver. This receiver utilizes multiple signals of the underwater acoustic field, i.e., its vector and scalar components. The vector components are the acoustic particle velocities in the *x* and *y* directions, whereas the scalar component is the acoustic pressure. Our measurements indicate that the multichannel vector receiver provides higher SNRs and lower correlations, compared to the conventional approach of using scalar sensor receivers. These can lead to stronger peaks at the output of the chirp matched filter, when the ring vector sensor is used. Overall, the ring vector receiver appears to be advantageous in underwater communication systems and applications.

References

[1] N. C. Beaulieu and D. J. Young, "Designing time-hopping ultrawide bandwidth receivers for multiuser interference environments," *Proc. IEEE*, vol. 97, pp. 255-284, 2009.

[2] M. S. Bashir and M.-S. Alouini, "Signal acquisition with photon-counting detector arrays in free-space optical communications," *IEEE Trans. Wireless Commun.*, vol. 19, pp. 2181-2195, 2020.

[3] S. Zhou and Z. Wang, *OFDM for Underwater Acoustic Communications*. Wiley, 2014.

[4] J.-H. Cui, J. Kong, M. Gerla, and S. Zhou, "The challenges of building scalable mobile underwater wireless sensor networks for aquatic applications," *IEEE Network*, vol. 20, no. 3, pp. 12-18, 2006.

[5] N. He and C. Tepedelenlioglu, "Joint pulse and symbol level acquisition of UWB receivers," *IEEE Trans. Wireless Commun.*, vol. 7, pp. 6-14, 2008.

[6] A. F. Molisch, *Wireless Communications*, 2nd ed. Wiley, 2011.

[7] G. L. Stuber, *Principles of Mobile Communication*, 4th ed. Springer, 2017.

[8] S. A. Saberali and N. C. Beaulieu, "Matched-filter detection of the presence of MPSK signals," in *Proc. Int. Symp. Inform. Theory Appl.*, Victoria, Australia, 2014, pp. 85-89.

[9] A. Abdi and H. Guo, "A new compact multichannel receiver for underwater wireless communication networks," *IEEE Trans. Wireless Commun.*, vol. 8, pp. 3326-3329, 2009.

[10] A. Nehorai and E. Paldi, "Acoustic vector-sensor array processing," *IEEE Trans. Signal Processing*, vol. 42, pp. 2481-2491, 1994.

[11] M. Hawkes and A. Nehorai, "Acoustic vector-sensor beamforming and Capon direction estimation," *IEEE Trans. Signal Process.*, vol. 46, pp. 2291-2304, 1998.

[12] X. Zhong, A. B. Premkumar and H. Wang, "Multiple wideband acoustic source tracking in 3-D space using a distributed acoustic vector sensor array," *IEEE Sens. J.*, vol. 14, no. 8, pp. 2502-2513, 2014.

[13] P. K. Tam, K. T. Wong and Y. Song, "An hybrid Cramér-Rao bound in closed form for direction-of-arrival estimation by an "acoustic vector sensor" with gain-phase uncertainties," *IEEE Trans. Signal Process.*, vol. 62, pp. 2504-2516, 2014.

[14] A. Weiss, "Blind direction-of-arrival estimation in acoustic vector-sensor arrays via tensor decomposition and Kullback-Leibler divergence covariance fitting," *IEEE Trans. Signal Process.*, vol. 69, pp. 531-545, 2021.

[15] J. He, M. N. S. Swamy and M. O. Ahmad, "Joint space-time parameter estimation for underwater communication channels with velocity vector sensor arrays," *IEEE Trans. Wireless Commun.*, vol. 11, pp. 3869-3877, 2012.

[16] K. Wang, J. He, T. Shu, and Z. Liu, "Joint angle and delay estimation for underwater acoustic multicarrier CDMA systems using a vector sensor," *IET Radar Sonar Navig.*, vol. 10, pp. 774-783, 2016.

[17] F. Fauziya, B. Lall and M. Agrawal, "Impact of vector sensor on underwater acoustic communications system," *IET Radar Sonar Navig*., vol. 12, pp. 1500-1508, 2018.

[18] X. Han, J. Yin, Y. Tian and X. Sheng, "Underwater acoustic communication to an unmanned underwater vehicle with a compact vector sensor array," *Ocean Engineering*, vol. 184, pp. 85-90, 2019.

[19] M. Rawat, B. Lall and S. Srirangarajan, "Statistical modeling and performance analysis of cooperative communication in frequency-selective underwater acoustic channel using vector sensor," *IEEE Sens. J.*, vol. 21, pp. 7367-7379, 2021.

[20] H. Saheban and Z. Kordrostami, "Hydrophones, fundamental features, design considerations, and various structures: A review," *Sensors and Actuators A: Physical*, vol. 329, 112790, 2021.

[21] A. G. Zajic, "Statistical modeling of MIMO mobile-to-mobile underwater channels," *IEEE Trans. Vehic. Technol.*, vol. 60, pp. 1337-1351, 2011.

[22] C. Chen and A. Abdi, "Signal transmission using underwater acoustic vector transducers," *IEEE Trans. Signal Process.*, vol. 61, pp. 3683-3698, 2013.

[23] C. Chen and A. Abdi, "A vector sensor receiver for chirp modulation in underwater acoustic particle velocity channels," in *Proc. Conf. Underwater Commun.: Channel Modelling Validation*, Sestri Levante, Italy, 2012, pp. 1-8.

[24] M. K. Simon and M.-S. Alouini, *Digital Communication over Fading Channels*, 2nd ed., Hoboken, NJ: Wiley, 2005.

[25] X. Zhang and N. C. Beaulieu, "Performance analysis of generalized selection combining in generalized correlated Nakagami-*m* fading," *IEEE Trans. Commun.*, vol. 54, pp. 2103- 2112, 2006.

[26] A. Abdi, H. Guo, A. Song and M. Badiey, "An overview of underwater acoustic communication via particle velocity channels: Channel modeling and transceiver design," in *Proc. Meetings on Acoustics (159th Meeting of Acoustical Society of America)*, Baltimore, MD, vol. 9, 2010, pp. 1-5.

[27] A. Abdi and H. Guo, "Signal correlation modeling in acoustic vector sensor arrays," *IEEE Trans. Signal Process.*, vol. 57, pp. 892-903, 2009.